This is an *Accepted Manuscript*, which has been through the Royal Society of Chemistry peer review process and has been accepted for publication.

Accepted Manuscripts are published online shortly after acceptance, before technical editing, formatting and proof reading. Using this free service, authors can make their results available to the community, in citable form, before we publish the edited article. We will replace this *Accepted Manuscript* with the edited and formatted *Advance Article* as soon as it is available.

You can find more information about *Accepted Manuscripts* in the **Information for Authors**.

Please note that technical editing may introduce minor changes to the text and/or graphics, which may alter content. The journal's standard **Terms & Conditions** and the **Ethical guidelines** still apply. In no event shall the Royal Society of Chemistry be held responsible for any errors or omissions in this *Accepted Manuscript* or any consequences arising from the use of any information it contains.

Graphical Abstract

Title: Chiral crystallization and optical properties of three metal complexes based on two non-centrosymmetric tripodal ligands

Authors: Ming-Dao Zhang,[a,b] Zhi-Qiang Shi,[b] Min-Dong Chen,[a] and He-Gen Zheng*[,b]
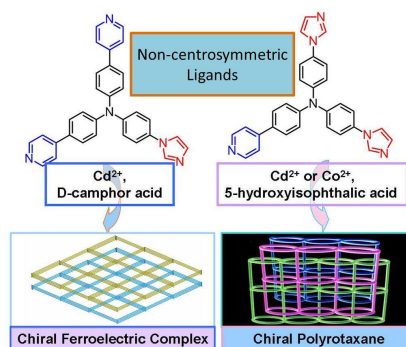
Three chiral coordination polymers **1-3** with novel architectures were constructed by asymmetric induction. Complex **3** can satisfy the fundamental requirement of ferroelectric and second-order nonlinear optical materials.

ARTICLE TYPE

Chiral crystallization and optical properties of three metal complexes based on two non-centrosymmetric tripodal ligands †

Ming-Dao Zhang,[a,b] Zhi-Qiang Shi,[b] Min-Dong Chen,[a] and He-Gen Zheng*[,b]

Chiral coordination polymers have attracted much attention due to their special properties and significant applications. In this work, we synthesized two non-centrosymmetric ligands, N,N-bis(4-(1H-imidazol-1-yl)phenyl)-4-(pyridin-4-yl)aniline (DIMPPA) and N-(4-(1H-imidazol-1-yl)phenyl)-4-(pyridin-4-yl)-N-(4-(pyridin-4-yl)phenyl)aniline (MIDPPA), *via* structural modification of two reported centrosymmetric
10 ligands; after that achiral → chiral induction occurred in the construction of three coordination polymers namely $\{[Cd(DIMPPA)(5–OH–bdc)](H_2O)\}_n$ (**1**), $\{[Co(DIMPPA)(5–OH–bdc)](H_2O)\}_n$ (**2**) and $\{[Cd_2(MIDPPA)_2(D–ca)_2(H_2O)_2](H_2O)_5\}_n$ (**3**), when replacing the reported centrosymmetric ligands with non-centrosymmetric ligands (5-OH-H_2bdc = 5-hydroxyisophthalic acid, D-H_2ca = D-camphoric acid). Isostructual complexes **1** and **2** exhibit chiral 2D → 3D frameworks with coexistence of polyrotaxane and
15 parallel polycatenation features. Complex **3** shows two-fold interpenetrating 3D chiral architecture with *cds*-type topology. The luminescent emissions of both complexes **1** and **3** are mostly assignable to the internal $\pi\rightarrow\pi*$ electron transition in DIMPPA and MIDPPA, respectively. Complex **3** can satisfy the fundamental requirement of second-order nonlinear optical materials.

Introduction

20 Over the recent three decades, there has been more and more interest in the fabrication of chiral coordination polymers due to their novel architectures and special properties, such as asymmetric catalysis, enantioselective separation, circular
25 dichroism and second-order nonlinear optical (NLO) properties.[1-5] These properties can provide significant applications in optical storage, information processing, telecommunication and chiral catalysis.[1,2] Previously, most chiral coordination polymers were synthesized by coordination of chiral ligands and metal ions,
30 while chiral coordination polymers based on non-centrosymmetric ligands were barely reported,[4,5] which restrained the development of theoretical studies and practical applications of chiral coordination polymers.

In the past five years, two ligands namely tris(4-(1H-imidazol-
35 1-yl)phenyl)amine[6-8] (TIPA, Scheme 1) and tris(4-(pyridin-4-yl)phenyl)amine[9,10] (TPPA, Scheme 1), have been investigated intensely in the field of functional coordination polymers. Dozens of complexes, featuring aesthetic structures or potential applications, have been constructed from TIPA or TPPA.
40 Notably, $\{[Cd(TPPA)(trans-chdc)]\}_n$[9] represents the first example of a 4-fold interpenetrating 3D metal-organic polyrotaxane framework; $\{[WOS_3Cu_3Br(TIPA)](H_2O)(DMF)\}_n$, a 3D cluster polymer, based on TIPA and Mo(W)/Cu/S cluster, exhibits strong third-order NLO properties.[8]

45 However, no coordination polymers based on TPPA or TIPA ligand is crystallized in non-centrosymmetric space group no matter if the co-ligands is chiral, which can be attributed to centrosymmetric feature of TPPA and TIPA. For instance, $\{[M(TIPA)_3(5-OH-bdc)_3]\cdot 2H_2O\}_n$ (M = Cd or Co, 5-OH-H_2bdc =
50 5-hydroxyisophthalic acid)[7,8] and $\{[Co(TPPA)_2(D-ca)_2]\cdot(H_2O)\}_n$[9] (D-$H_2$ca = D-camphoric acid) crystallize in monoclinic space group $P2_1/n$ and triclinic space group $P\bar{1}$, respectively.
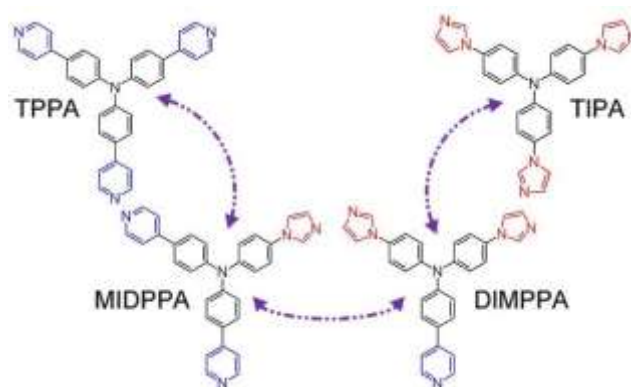
55 **Scheme 1.** Structures of TPPA, TIPA, DIMPPA and MIDPPA.

Inspired by the chiral induction function of non-centrosymmetric ligands,[11] we replaced an imidazolyl group of TIPA with a pyridyl group, or replaced a pyridyl group of TPPA
60 with an imidazolyl group, to design two non-centrosymmetric

ligands, N,N-bis(4-(1H-imidazol-1-yl)phenyl)-4-(pyridin-4-yl)aniline (DIMPPA, Schemes 1 and 2) N-(4-(1H-imidazol-1-yl)phenyl)-4-(pyridin-4-yl)-N-(4-(pyridin-4-yl)phenyl)aniline (MIDPPA, Schemes 1 and 2), respectively.

5   In order to test the chiral induction abilities of DIMPPA and MIDPPA, we adopted 5-OH-H_2bdc[12] and D-H_2ca[13] as co-ligands again to coordinate with DIMPPA (or MIDPPA) and different bivalent metal salts. Then, three chiral coordination polymers, namely {[Cd(DIMPPA)(5–OH–bdc)](H_2O)}$_n$ (**1**),
10 {[Co(DIMPPA)(5–OH–bdc)](H_2O)}$_n$ (**2**) and {[Cd_2(MIDPPA)$_2$(D–ca)$_2$(H_2O)$_2$](H_2O)$_5$}$_n$ (**3**), were obtained under solvothermal conditions. Three complexes were characterized by X-ray crystallography IR spectra, elemental analysis, and X-ray powder diffraction experiment [9-11].
15 Meanwhile, topological analyses of **1**-**3**, solid-state photoluminescence and the emission decay lifetimes of **1**, **3** and ligands, dielectric behavior and second-order nonlinear optical effect of **3** are also presented.

Experimental Section

20 **Materials and General Methods**

IR spectra of the complexes were recorded on a Nicolet (Impact 410) spectrometer with KBr pellets (3 mg of sample in 300 mg of KBr) in the range of 400–4000 cm^{-1}. Using a Philip X' Pert Pro system, variable temperature PXRD (VT-PXRD) measurements
25 were recorded after the samples had stayed at the room temperature for 30 min in N_2 atmosphere. C, H and N element analysis was operated with a Perkin Elmer 240C elemental analyzer. The as-synthesized complexes were characterized by thermo analysis (TGA) on a Perkin Elmer thermogravimetric
30 analyzer Pyris 1 TGA up to 700 K using a heating rate of 10 K min^{-1} under a N_2 atmosphere. The SHG measurements were done on sieved powders with particle size between 200 and 250 nm. Second-order NLO properties are studied using a pulsed Q-switched Nd:YAG laser at a wavelength of 1064 nm as SHG
35 signals. The electric hysteresis loops were recorded on a Ferroelectric Tester PrecisionPremier II made by Radiant Technologies, Inc.

Syntheses of Ligands MIDPPA and DIMPPA

Synthesis of 4-bromo-*N*,*N*-bis(4-(pyridin-4-yl)phenyl) aniline
40 **(I) and 4-bromo-N-(4-bromophenyl)-N-(4-(pyridin-4-yl)phenyl)aniline (II).** Pyridine-4-boronic acid (1.85 g, 15.0 mmol), Pd(PPh)$_4$ (231 mg, 0.20 mmol), 4,4′,4″-tribromotriphenylamine (4.82 g, 10.0 mmol), 1,4-dioxane (100 mL) and 0.5 M K_2CO_3 (aq) (50 mL) were mixed and refluxed for
45 24 hours under argon. After cooling to room temperature, the reaction mixture was extracted by CHCl$_3$ (3 × 150mL). The organic layers were all combined, dried and evaporated in vacuo. The residue was purified with column chromatography (silica gel, EtOAc as eluent) to give target compounds **I** (2.05 g, yield 43%)
50 and **II** (1.90 g, yield 40%). ^{1}H NMR for **I** (DMSO–d_6, 500 MHz, Fig S1, ESI†): δ, [ppm]: 7.10 (d, J = 9.0 Hz, 2H), 7.19 (d, J = 8.5 Hz, 4H), 7.56 (d, J = 8.5 Hz, 2H), 7.70 (d, J = 6.0 Hz, 4H), 7.82 (d, J = 8.5 Hz, 4H), 8.62 (d, J = 6.0 Hz, 4H). ^{13}C NMR for **I** (DMSO–d_6, 125 MHz, Fig S2, ESI†): δ, [ppm]: 116.35, 121.12,
55 124.46, 127.11, 128.61, 132.15, 133.11, 146.22, 146.71, 147.91, 150.60. MS (MALDI –Tof) for **I**: Calcd for $C_{28}H_{20}BrN_3$, 478.39;

found, 478.417. ^{1}H NMR for **II** (CDCl$_3$, 500 MHz, Fig S3, ESI†): δ, [ppm]: 7.01 (d, J = 8.5 Hz, 4H), 7.15 (d, J = 8.5 Hz, 2H), 7.41 (d, J = 8.5 Hz, 4H), 7.49 (d, J = 3.5 Hz, 2H), 7.56 (d, J = 8.5 Hz,
60 2H), 8.65 (s, 2H). ^{13}C NMR for **II** (CDCl$_3$, 125 MHz, Fig S4, ESI†): δ, [ppm]: 116.47, 121.01, 123.72, 126.13, 128.00, 132.35, 132.62, 146.02, 147.42, 147.97, 150.21. MS (EI–MS) for **II**: Calcd for $C_{23}H_{16}Br_2N_2$, 477.97; found, 478.76 {[M+H]$^+$}.

65
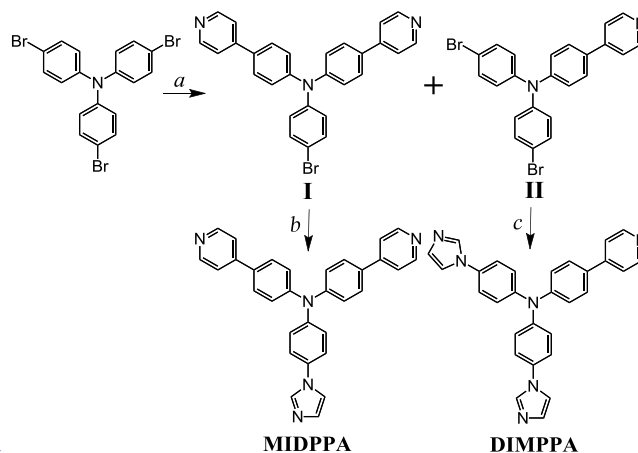
Scheme 2. Synthetic steps of MIDPPA and DIMPPA. Conditions and reagents: (*a*) Pd(PPh)$_4$, Pyridine-4-boronic acid, 1,4-dioxane, 0.5 M K_2CO_3(aq), refluxed, 24 h; (*b*) Cu_2O, $CuSO_4$, imidazole, K_2CO_3, DMF,
70 150 °C, 48 h; (*c*) Cu_2O, $CuSO_4$, imidazole, K_2CO_3, DMF, 150 °C, 72 h.

Synthesis of N-(4-(1*H*-imidazol-1-yl)phenyl)-4-(pyridin-4-yl)-N-(4-(pyridin- 4-yl) phenyl)aniline (MIDPPA). Cu_2O (14.3 mg, 0.10 mmol), 4-bromo-N-(4-bromophenyl)-N-(4-(pyridin-4-
75 yl)phenyl)aniline (2.39 g, 5.0 mmol), imidazole (6.80 g, 100.0 mmol), K_2CO_3 (6.90 g, 50.0 mmol), $CuSO_4$ (16.0 mg, 0.10 mmol) and DMF (5.0 mL) were mixed and heated at 150 °C for 48 h under argon. The mixture was then cooled to room temperature, poured into 250 mL water and extracted with CHCl$_3$ (3 × 100
80 mL). The organic layers were all combined, dried and evaporated in vacuo. The residue was purified with column chromatography (silica gel, EtOAc/MeOH = 10/1 as eluent) to give yellow solid (2.02 g, yield 87%). ^{1}H NMR (CDCl$_3$, 500 MHz, Fig S5, ESI†): δ, [ppm]: 7.26 (d, J = 8.5 Hz, 4H), 7.28-7.40 (m,4H), 7.36 (d, J =
85 9.0 Hz, 2H), 7.51 (d, J = 4.5 Hz, 4H), 7.62 (d, J = 8.5 Hz, 4H), 7.88 (s, 1H), 8.66 (s, 4H). ^{13}C NMR (CDCl$_3$, 125 MHz, Fig S6, ESI†): δ, [ppm]: 118.38, 121.05, 122.86, 124.42, 125.79, 128.12, 132.42, 132.90, 133.03, 135.67, 146.32, 147.37, 147.88, 150.26. MS (MALDI -Tof): MS (EI–MS): Calcd for $C_{31}H_{23}N_5$, 465.20;
90 found, 466.41 {[M+H]$^+$}.

Synthesis of N,N-bis(4-(1H-imidazol-1-yl)phenyl)-4-(pyridin-4-yl)aniline (DIMPPA). A mixture of $CuSO_4$ (32.0 mg, 0.20 mmol), 4-bromo-*N*,*N*-bis(4-(pyridin-4-yl)phenyl)aniline (2.39 g, 5.0 mmol), imidazole (13.60 g, 200.0 mmol), K_2CO_3
95 (13.80 g, 100.0 mmol), Cu_2O (28.6 mg, 0.20 mmol) and DMF (10.0 mL) was heated at 150 °C for 72 h under argon. The mixture was then cooled to room temperature, poured into 300 mL water and extracted with CHCl$_3$ (3 × 200 mL). The organic layers were all combined, dried and evaporated in vacuo. The
100 residue was purified with column chromatography (silica gel, EtOAc/MeOH = 10/1 as eluent) to give pale yellow solid (1.55 g,

yield 68%). ^{1}H NMR (CDCl$_3$, 500 MHz, Fig S7, ESI†): δ, [ppm]: 7.20–7.30 (m, 10H), 7.35 (d, J = 8.5 Hz, 4H), 7.51 (d, J = 6.0 Hz, 2H), 7.62 (d, J = 8.5 Hz, 2H), 7.86 (s, 2H), 8.66 (d, J = 5.5 Hz, 2H). ^{13}C NMR (CDCl$_3$, 125 MHz, Fig S8, ESI†): δ, [ppm]: 118.33, 121.03, 122.90, 124.12, 125.50, 128.17, 130.44, 132.91, 133.00, 135.64, 146.31, 147.32, 147.87, 150.29. MS (EI–MS): Calcd for C$_{29}$H$_{22}$N$_6$, 454.19; found, 455.17 {[M+H]$^+$}.

Syntheses of the complexes 1–3

Synthesis of {[Cd(DIMPPA)(5–OH–bdc)](H$_2$O)}$_n$ (1). Cd(NO$_3$)$_2$·4H$_2$O (15.1 mg, 0.05 mmol), DIMPPA (22.7 mg, 0.05 mmol), and 5-hydroxyisophthalic acid (9.1 mg, 0.05 mmol) was dissolved in 12 mL of DMF / MeCN / H$_2$O (1 / 1 / 2, v / v). The mixture was placed in a Parr Teflon-lined stainless steel vessel (20 mL) under autogenous pressure and heated at 100 °C for 3 d. Yellow crystals was obtained, which were washed with mother liquid, and dried under ambient conditions (yield: 65%, based on DIMPPA). Calcd for CdC$_{37}$H$_{28}$N$_6$O$_6$: C, 58.09%; H, 3.69%; N, 10.98%. Found: C, 58.18%; H, 3.66%; N, 10.91%. IR (KBr, cm^{-1}): 3299 (s), 1599 (s), 1568 (s), 1520 (m), 1488 (s), 1370 (s), 1286 (m), 1243 (m), 1227 (w), 1187 (w), 1121 (m), 1093 (w), 1062 (s), 1004 (w), 978 (w), 965 (m), 930 (w), 880 (w), 818 (s), 780 (m), 735 (s), 655 (m), 545 (m).

Synthesis of {[Co(DIMPPA)(5–OH–bdc)](H$_2$O)}$_n$ (2). Synthetic procedure of **2** is similar to that of **1**, while Cd(NO$_3$)$_2$·4H$_2$O was replaced with Co(NO$_3$)$_2$·6H$_2$O (14.6 mg, 0.05 mmol). Red crystals was obtained (yield: 66%, based on DIMPPA). Calcd for CoC$_{37}$H$_{30}$N$_6$O$_7$: C, 60.91%; H, 4.14%; N, 11.52%. Found: C, 60.80%; H, 4.16%; N, 11.60%. IR (KBr, cm^{-1}): 3263 (s), 1600 (s), 1573 (s), 1518 (m), 1489 (s), 1370 (s), 1321 (s), 1283 (s), 1241 (m), 1121 (w), 1063 (s), 965 (m), 819 (s), 778 (s), 735 (s), 659 (m), 545 (m).

Synthesis of {[Cd$_2$(MIDPPA)$_2$(D–ca)$_2$(H$_2$O)$_2$](H$_2$O)$_5$}$_n$ (3). Cd(NO$_3$)$_2$·4H$_2$O (15.1 mg, 0.05 mmol), MIDPPA (23.3 mg, 0.05 mmol), and D-camphoric acid (10.0 mg, 0.05 mmol) was dissolved in 12 mL of DMA / H$_2$O (1 / 1, v / v). The mixture was placed in a Parr Teflon-lined stainless steel vessel (20 mL) under autogenous pressure and heated at 120 °C for 3 d. Yellow crystals was obtained, which were washed with mother liquid, and dried under ambient conditions (yield: 53%, based on MIDPPA). Calcd for Cd$_2$C$_{82}$H$_{88}$N$_{10}$O$_{14}$: C, 59.24%; H, 5.34%; N, 8.43%. Found: C, 59.22%; H, 5.39%; N, 8.36%. IR (KBr, cm^{-1}): 3384 (s), 2968 (w), 1649 (w), 1596 (s), 1518 (s), 1489 (s), 1398 (m), 1363 (w), 1323 (s), 1294 (s), 1228 (w), 1185 (w), 1124 (w), 1067 (m), 997 (w), 964 (w), 931 (w), 818 (s), 750 (m), 731 (w), 653 (w), 569 (w), 518 (m).

Single crystal structure determination and refinement

X-ray crystallographic data of **1-3** were collected at room temperature by way of sealing the better single crystals in a quartz tube with mother liquor. X-ray crystallographic data of these complexes were collected on a Bruker Apex Smart CCD diffractometer with graphite-monochromated Mo-K$_\alpha$ radiation (λ = 0.71073 Å). A semiempirical absorption correction was applied (SADABS), and the program SAINT was used for integration of the diffraction profiles.[14] Structure solutions were solved by direct methods and the non-hydrogen atoms were located from the trial structures and then refined anisotropically with *SHELXTL* using full-matrix least-squares procedures based on F^2

values.[15] The hydrogen atom positions were fixed geometrically at calculated distances and allowed to ride on the parent atoms. The topological analyses carried out with Topos 40 program.[16-19] The crystal parameters of **1-3** are listed in Table 1. The selected bond lengths and angles are summarized in Tables S1 (ESI†). CCDC numbers are 1013987−1013989 for **1−3**, respectively.

Table 1. Crystallographic data and structure refinement details for complexes **1-3**.

Complexes	1	2	3
Formula	C$_{37}$H$_{28}$CdN$_6$O$_6$	C$_{37}$H$_{28}$CoN$_6$O$_6$	C$_{82}$H$_{88}$Cd$_2$N$_{10}$O$_{14}$
Formula Weight	765.05	729.60	1662.42
Crystal System	Orthorhombic	Orthorhombic	Triclinic
Space group	$P2_12_12_1$	$P2_12_12_1$	$P1$
a (Å)	10.005(3)	9.734(5)	10.971(3)
b (Å)	18.631(6)	18.245(9)	12.137(3)
c (Å)	19.444(6)	19.123(10)	15.696(4)
α (deg)	90.00	90.00	89.991(2)
β (deg)	90.00	90.00	90.030(1)
γ (deg)	90.00	90.00	112.009(3)
V (Å^3)	3624.4(19)	3396(3)	1937.8(9)
Z	4	4	1
D$_c$ (g cm^{-3})	1.402	1.427	1.425
μ(Mo Ka)(mm^{-1})	0.655	0.565	0.620
F(000)	1552	1508	858
θ$_{min–max}$ (deg)	1.51, 25.00	1.54, 25.00	1.81, 25.00
Tot., Uniq. Data	24642, 6352	13176, 5839	9757, 8167
R(int)	0.1016	0.0998	0.1146
Observed data [$I > 2\sigma(I)$]	6352	5839	8167
R1,wR2[I> 2σ(I)]	0.0610, 0.1569	0.0758, 0.1582	0.0706, 0.1836
S	1.080	1.001	1.011
Min. and max	−1.196, 0.893	−0.706, 0.841	−1.458, 1.260

$R1 = \Sigma||F_o|-|F_c||/\Sigma|F_o|$. w$R2 = \{\Sigma[w(F_o^2-F_c^2)^2]/\Sigma[w(F_o^2)^2]\}^{1/2}$; where w = $1/[\sigma^2(F_o^2)+(aP)^2+bP]$, $P = (F_o^2+2F_c^2)/3$

Results and Discussion

Description of the crystal structures

{[Cd(DIMPPA)(5–OH–bdc)](H$_2$O)}$_n$ (1). X-ray crystallography[14-20] reveals that complex **1** crystallizes in chiral orthorhombic crystal system of $P2_12_12_1$. The Flack parameter of **1** is 0.05(2). The local coordination environment around the Cd^{2+} atom is depicted in Fig. 1. Each Cd atom in **1** coordinates to two N atoms from two imidazolyl groups of two DIMPPA molecules, one N atom from one pyridyl group of one DIMPPA molecule, and four oxygen atoms from two distinct deprotonated 5–OH–bdc^{2-} anions with chelate coordination mode. The Cd-O lengths are in the range of 2.267(2)-2.471(2) Å and Cd-N lengths are in

the range of 2.306(3)-2.355(3) Å, which are all similar to the values found in {[Cd(TIPA)(5-OH-bdc)]·2H$_2$O}$_n$.[3b]

For each triphenylamine moiety in **1**, the dihedral angles between phenyl rings are 66.479°, 69.713° and 67.165°, demonstrating the propeller-like structure. For each DIMPPA molecule in **1**, the dihedral angle between pyridyl and adjacent phenyl rings is 34.674°, while the dihedral angles between imidazolyl and nearby phenyl rings are 41.874° and 46.130°. In **1**, each DIMPPA molecule coordinates to three Cd atoms, forming a 1D ladderlike chain (Fig. 2a). The length between central nitrogen atom N6 and adjacent Cd atoms are 9.794 Å, 9.854 Å and 10.781 Å. Each two nearby ladderlike chains are linked by 5–OH–bdc^{2-} anions, giving rise to a 2D network (Figs. 2b and 2c). There is a kind of channels with a cross section of approximately 10.7 × 13.8 Å in the single network of **1** (Fig. 2b, excluding Vander Waals radii). Packing drawing of **1** gives two sets of networks. Each two adjacent networks from one set are entangled by network from another set, further forming 2D→3D structure of **1** *via* parallel polycatenation (Fig. 2d).
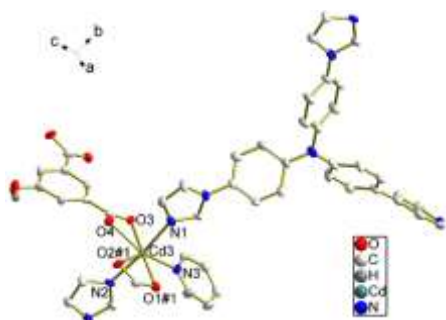
Fig. 1. Coordination geometry of Cd^{2+} atom in **1**. The hydrogen atoms are omitted for clarity (30% ellipsoid probability). Symmetry code: #1 = 1+*x*, *y*, *z*.
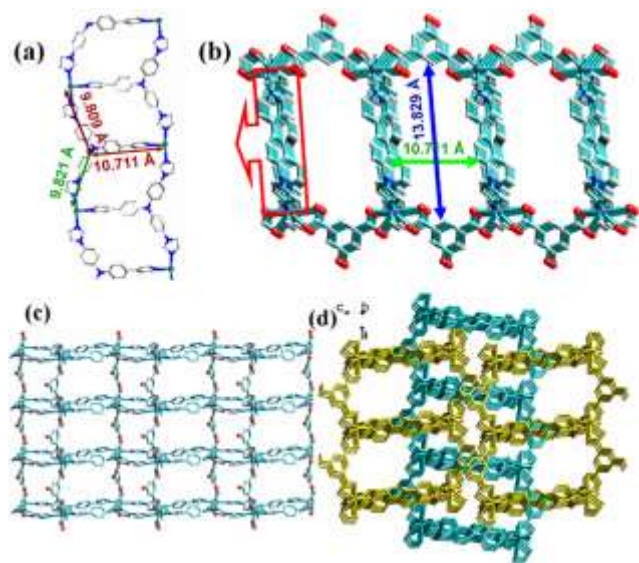
Fig. 2. (a) 1D chains constructed by DIMPPA and Cd^{2+} atoms in **1**; (b) Single network of **1** along the *b* axis; (c) A view of Single network of **1** along the *c* axis; (d) 2D→3D structure of **1** *via* parallel polycatenation.
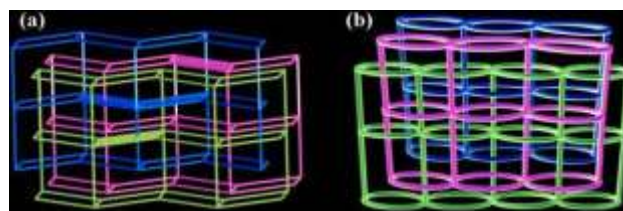
Fig. 3. (a) Simplified structure of **1**; (b) A schematic representation of 2D→3D polyrotaxane framework.

From the topological point, we can view the structure of **1** more clearly.[12] Each Cd atom can be can be simplified as 5-connecting node; each 5–OH–bdc^{2-} anion and DIMPPA molecule in tridentate mode can be considered as linker and 3-connecting node, respectively. Then, the single network of **1** can be viewed as 3,5L2 network (Fig. 3a), and the Schläfli symbol for this binodal net is {4^2.6^7.8^3}{4^2.6}.

The grids of ladder-like chains can be considered as successions of loops, while 5–OH–bdc^{2-} anions can be viewed as rods. We can find that each loop is threaded by a rod, indicating that complex **1** possesses the highly rare fascinating chiral 2D→3D polyrotaxane characters (Fig. 3b).[21]

{[Co(DIMPPA)(5–OH–bdc)](H$_2$O)}$_n$ (2). The crystal structure determination[14-20] reveals that complex **2** also crystallize in chiral orthorhombic crystal system of $P2_12_12_1$ with the Flack parameter as 0.07(3). The Co-O lengths are in the range of 2.059(5)-2.271(17) Å and Cd-N lengths are in the range of 2.099(5)-2.156(6) Å, which are all close to the values found in {[Co(TIPA)(5-OH-bdc)]·2H$_2$O}$_n$.[6] There is no obvious difference of the crystallographic data and coordination modes (Fig. 1) of metal atoms in **1** and **2**. Complexes **1** and **2** are isostructural despite of using different metal salts,[22] therefore we do not discuss crystal structure of **2** further more.

{[Cd$_2$(MIDPPA)$_2$(D–ca)$_2$(H$_2$O)$_2$](H$_2$O)$_5$}$_n$ (3). X-ray analysis[14-20] reveals that **3** crystallized in triclinic space group $P1$. The Flack parameter of **3** is 0.02(3). The asymmetric unit of **3** contains two Cd(II) cations, two D-Camphoric acid anions, two MIDPPA molecules, two coordinated water molecules, and five lattice water molecules.
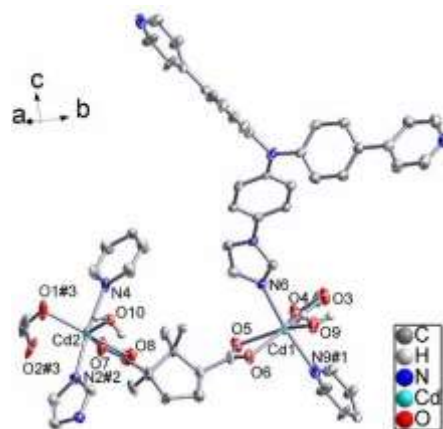
Fig. 4. Coordination geometry of Cd^{2+} atom in **3**. Most hydrogen atoms are omitted for clarity (30% ellipsoid probability). Symmetry code: #1 = −1+*x*, *y*, −1+*z*; #2 = 1+*x*, *y*, −1+*z*; #3 = 1+*x*, −1+*y*, *z*.

As shown in Fig. 4, Cd1 and Cd2 are both coordinated with two carboxylic groups from two D-Camphoric acid molecules,

one O atom from one coordinated water molecule, one nitrogen atom from one pyridyl group in one MIDPPA molecule and one nitrogen atom from one imidazolyl group in another MIDPPA molecule. In each asymmetric unit of **3**, one carboxylic group (O1-C49-O2) adopts monodentate coordination mode, while the other three carboxylic groups adopt chelate coordination bonding mode. Therefore, Cd1 and Cd2 are 7-coordinated and 6-coordinated respectively. The Cd-O lengths are in the range of 2.206(7)-2.590(5) Å and Cd-N lengths are in the range of 2.294(5)–2.369(6) Å, which are all similar to the values found in other Cd(II) complexes.[23]

Fig. 5. (a) 1D chain constructed from Cd atoms and MIDPPA ligands in **3**; (b) 1D chain constructed from Cd atoms and D-Camphoric acid anions.
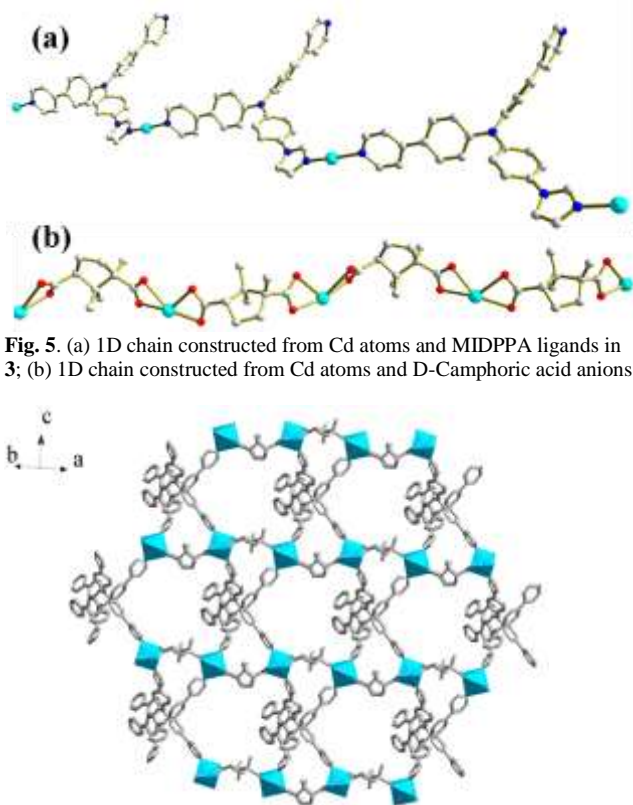
Fig. 6. Single 3D framework of **3**.

For one triphenylamine moiety in **3**, the dihedral angles between phenyl rings are 61.157°, 70.680° and 85.235°, and for another triphenylamine moiety in **3** the angles are 63.906°, 67.037° and 80.504°, demonstrating the propeller-like structure of MIDPPA molecules.[24] For each MIDPPA molecule in **3**, the dihedral angle between imidazolyl and adjacent phenyl rings are 36.058° and 35.953°, while the dihedral angles between pyridyl and nearby phenyl rings are 10.255°, 21.583°, 25.455°, and 37.196°.

For each MIDPPA molecule in **3**, one pyridyl N atom is free, while another pyridyl N atom and imidazolyl N atom coordinate to Cd atoms (Fig. 5a), forming a kind of chains. The length between central nitrogen atoms (N1 and N8) and adjacent Cd atoms are 9.614 Å, 9.607 Å, 10.832 Å and 10.787 Å. Each D-Camphoric acid anion also coordinates to two Cd atoms (Fig. 5b), forming another kind of chains. Different chains share Cd atoms with each other, giving rise to a 3D framework, as shown in Fig. 6.
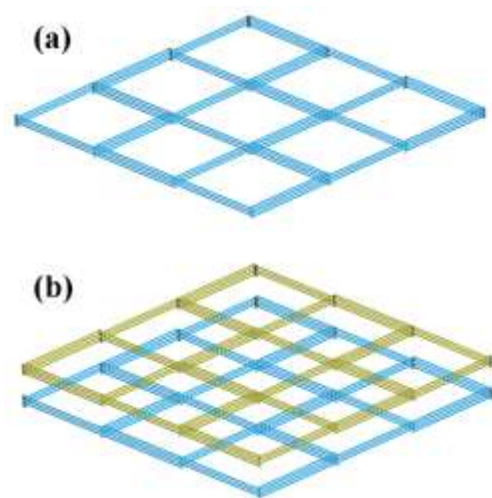
Fig. 7. (a) Single simplified framework of **3**; (b) Two-fold interpenetrating 3D ***cds***-type topology of **3**.

The 3D frameworks of **3** can be viewed more clearly by the topological method. The Cd atom can be regarded as a four-connected node, D-Camphoric acid anions and two MIDPPA molecules can be considered as linkers, thus forming a 4-connected network (Fig. 7a). Packing drawing of the simplified frameworks gives two-fold interpenetrating 3D ***cds***-type topology of **3**. (Fig. 7b). The Schläfli symbol for this binodal net is $\{6^5.8\}$. According to a calculation performed using PLATON, complex **3** contains a solvent accessible void space of 9.6% of the total crystal volume.

Second-order Nonlinear Optical (NLO) Property of $\{[Cd_2(MIDPPA)_2(D–ca)_2(H_2O)_2](H_2O)_5\}_n$ (3).

The nonlinear optical (NLO) property is significant in the emerging field of photonics, in which photons instead of electrons are used for signal processing and transmission.[25-28] One of the most common NLO behaviors is second-harmonic generation (SHG). Complex **3** is acentric with a chiral space groups (*P*1). Hence, its second-order NLO property is worth studying. A pulsed Q-switched Nd:YAG laser at a wavelength of 1064 nm was used to generate a SHG signal. The result of SHG measurements reveals that complex **3** display strong SHG response and the SHG efficiencies is 0.8 time that of urea crystal (SHG efficiency of urea equals to 20 times that of KDP and an efficiency of 320 times that of α-quartz).[28]

Dielectric Behavior of $\{[Cd_2(MIDPPA)_2(D–ca)_2(H_2O)_2](H_2O)_5\}_n$ (3).

Ferroelectric materials are vital physical properties in areas such as laser medicine, signal processing, optical communication, and the expanding field of integrated optical properties.[29] Especially, coordination polymers only crystallized in specific space groups or point groups (C_1, C_s, C_2, C_{2v}, C_3, C_{3v}, C_4, C_{4v}, C_6, C_{6v} or *1*, *2*, *3*, *4*, *6*, *m*, *mm2*, *3m*, *4mm*, *6mm*) can satisfy the requirement of ferroelectric materials.[30]

Space group (*P*1) of complex **3** is associated with the point group of C_1, one of the 10 polar point groups, indicating the potential to display ferroelectric behaviour. Thus, the electrical hysteresis loop of complex **3** was recorded at room temperature using crystal sample plates (Fig. 8).[31] The resulting curve of

complex **3** shows an electric hysteresis loops with a remnant electric polarization (P_r) of 0.018 μC/cm^2, and an electric coercive field (E_c) of 1.135 kV/cm with applying field up to ± 20 kV/cm; the spontaneous saturation polarization (P_s) of complex **3** is ca. 0.025 μC/cm^2. The loops in Fig. 8 indicates complex **3** is a leaky dielectric and not ferroelectric.[32]
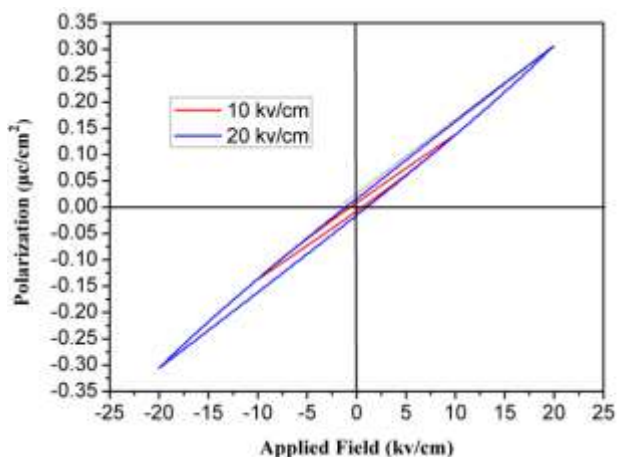
Fig. 8. Polarization versus applied electric field curves (electric hysteresis loops) of complex **1** under applying electric fields.

Photophysical Properties of {[Cd(DIMPPA)(5–OH–bdc)](H$_2$O)}$_n$ (1) and {[Cd$_2$(MIDPPA)$_2$(D–ca)$_2$(H$_2$O)$_2$](H$_2$O)$_5$}$_n$ (3).

Luminescent materials attract great attention due to their various appliatoms in light-emitting diodes (LEDs), chemical sensor, and photochemistry.[33] Complexes **1** and **3** are insoluble in regular organic solvents, hence photoluminescence properties of **1**, **3** and free DIMPPA and MIDPPA ligands were investigated in the solid state at room temperature (Fig. 9).

As shown in Fig. 9, DIMPPA exhibits two emission peaks in the ranges of 420 nm–490 nm (λ_{max} = 440 nm) and 490 nm–600 nm (λ_{max} = 520 nm) upon excitation at 405 nm. Similarly, MIDPPA also features two emission peaks in 420 nm–490 nm (λ_{max} = 455 nm) and 490 nm–600 nm (λ_{max} = 530 nm) upon excitation at 420 nm. For DIMPPA and MIDPPA, the emission in 420 nm–490 nm can be assigned to the $\pi \rightarrow \pi^*$ electron transition between imidazolyl groups and triphenylamine moiety, while the emission in 490 nm–600 nm is originated from the $\pi \rightarrow \pi^*$ electron transition between pyridyl groups and triphenylamine moiety. The peak heights are corresponding to the ratios of imidazolyl and pyridyl groups for DIMPPA and MIDPPA.

Complex **1**, containing DIMPPA, exhibits strong emission in 420 nm–600 nm (λ_{max} = 463 nm upon excitation at 406 nm), which is red-shifted by 23 nm compared with the stronger emission peak of DIMPPA. The red-shift of emission of **1** may be ascribed to the π-π interactions between DIMPPA molecules in **1**.[34,35]

Complex **3** based on MIDPPA, features strong emission in 450 nm–600 nm (λ_{max} = 520 nm upon excitation at 425 nm), which is blue-shifted by 10 nm compared with the stronger emission peak of MIDPPA. The blue-shift of emission of **3** may be ascribed to the weak $\pi \rightarrow \pi^*$ transitions of the MIDPPA molecules and D-Camphoric acid anions upon metal coordination.
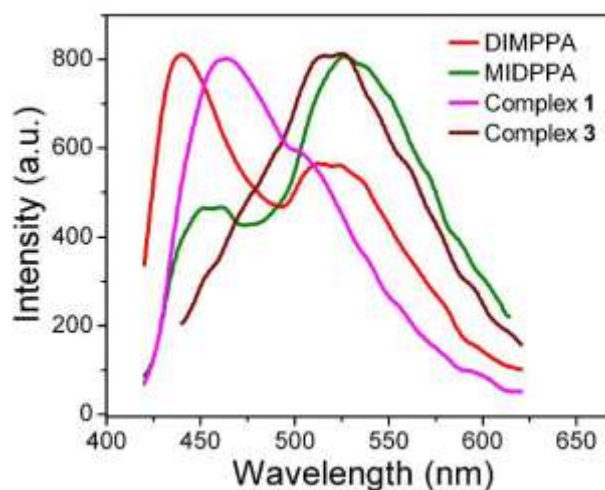
Fig. 9. Emission spectra of free TPPA ligand, complexes **1** and **3** in the solid state at room temperature.

Table 2. Detailed parameters from photophysical properties of **1**, **3** and free ligands.[a]

Sample	λ_{ex} /nm	λ_{em} /nm [Lifetime^a/ns (Rel)]
DIMPPA	405	440 [1.40 (100.00%)], 520 [3.29 (52.95%), 15.49 (47.05%)]
MIDPPA	420	455 [0.72 (76.81%), 2.24 (23.19%)], 530 [2.08 (59.02%), 14.03 (40.98%)]
1	406	463 [2.41 (100.00%)]
3	425	520 [1.64 (50.97%), 5.14 (49.03%)]

[a] The luminescent decay curves were fitted with a double-exponential decay function: Fit = A + B$_1$ × exp(-t / τ_1) + B$_2$ × exp(-t / τ_2).

Furthermore, the emission decay lifetimes of **1**, **3** and free ligands were monitored. The luminescent decay curves (Figs. S9-S14, ESI†) can be fitted with a double-exponential decay function. The results are summarized in Table 2. For both of DIMPPA and MIDPPA, emissions between 500-600 nm are longer than emissions between 400-500 nm. For complex **1**, the emission lifetime value falls in between the lifetimes of two emissions of DIMPPA. Similarly, for complex **2**, the emission lifetime value falls in between the lifetimes of two emissions of MIDPPA. The results indicate that the emissions of **1** and **3** can be mostly attributed to the charge transfer of internal DIMPPA and MIDPPA ligand, respectively.

PXRD and Thermal Analysis

To confirm whether the crystal structures are truly representative of the bulk materials tested in photochemical studies, PXRD experiment were carried out for complexes **1-3**. The PXRD experimental and computer-simulated patterns of the complexes **1-3** are shown in the Supporting Information, Figs. S15-S17 (ESI†), and they show that the bulk synthesized materials and the measured single crystals for **1-3** are the same.

To estimate the stability of the coordination architectures, thermal behaviors of complexes **1-3** were studied by thermogravimetric analysis (TGA) in N$_2$ atmosphere (Fig. S18, ESI†). For **1**, the first weight loss of 2.32% is observed from 40 to 150 °C, corresponding to the departure of the lattice water (calcd 2.35%). After the plateau between 150 to 320 °C, the decomposition of **1** occurred. For **2**, the first weight loss of 2.43%

is observed from 45 to 150 °C, corresponding to the departure of the lattice water (calcd 2.47%). After the plateau between 150 to 300 °C, the decomposition of **2** occurred. For **3**, the first weight loss of 5.46% is observed from 50 to 125 °C, corresponding to the departure of the lattice water (calcd 5.41%); the second weight loss of 2.10% is observed from 130 to 195 °C, corresponding to the departure of the coordinated water (calcd 2.16%). The network of complex **3** was decomposed quickly after 450 °C.

Conclusions

In summary, as we expected, the self-assembly of non-centrosymmetric ligand and carboxylate ligands is an effective method to generate aesthetic chiral architectures and topologies. In this work, we designed and synthesized two asymmetric N-containing ligands (DIMPPA or MIDPPA), and three new chiral coordination polymers were successfully synthesized based on DIMPPA (or MIDPPA) and carboxylate ligands. Complexes **1-3** exhibit interesting architectures and properties: 1) isostructual complexes **1** and **2** exhibit chiral 2D → 3D frameworks with coexistence of parallel polycatenation and polyrotaxane characters; 2) Complex **3** can satisfy the fundamental requirement of second-order nonlinear optical materials.

Acknowledgements

Notes and references

a Jiangsu Key Laboratory of Atmospheric Environment Monitoring and Pollution Control, Collaborative Innovation Center of Atmospheric Environment and Equipment Technology, School of Environmental Science and Engineering, Nanjing University of Information Science & Technology, Nanjing 210044, P. R. China. E-mail: matchlessjimmy@163.com.
b State Key Laboratory of Coordination Chemistry, School of Chemistry and Chemical Engineering, Nanjing National Laboratory of Microstructures, Nanjing University, Nanjing 210093, P. R. China, E-mail: zhenghg@nju.edu.cn. Fax: +86-25-83314502.

† Electronic supplementary information (ESI) available: X-ray crystallographic data in CIF format, Selected bond lengths and angles, luminescent emission decay curves, PXRD and TGA curves for complexes **1-3**. CCDC: 1013987—1013989 for complexes **1-3**. For ESI and crystallographic data in CIF or other electronic format see DOI: 10.1039/b000000x/

1. M. Yoon, R. Srirambalaji and K. Kim, *Chem. Rev.*, 2012, **112**, 1196-1231.
2. B. Kesanli and W. B. Lin, *Coord. Chem. Rev.*, 2003, **246**, 305-326.
3. G. Li, W. Yu, J. Ni, T. Liu, Y. Liu, E. Sheng and Y. Cui, *Angew. Chem. Int. Ed.*, 2008, **47**, 1245-1249.
4. E. Q. Gao, Y. F. Yue, S. Q. Bai, Z. He and C. H. Yan, *J. Am. Chem. Soc.*, 2004, **126**, 1419-1429.
5. L. Han and M. Hong, *Inorg. Chem. Commun*, 2005, **8**, 406-419.
6. X. Q. Yao, D. P. Cao, J. S. Hu, Y. Z. Li, Z. J. Guo and H. G. Zheng, *Cryst. Growth Des.*, 2011, **11**, 231-239.
7. H. Wu, H. Y. Liu, B. Liu, J. Yang, Y. Y. Liu, J. F. Ma, Y. Y. Liu and H. Y. Bai, *CrystEngComm*, 2011, **13**, 3402-3047.
8. X. Q. Yao, Z. R. Pan, J. S. Hu, Y. Z. Li, Z. J. Guo and H.G. Zheng, *Chem. Commun.*, 2011, 10049-10051.
9. M. D. Zhang, C. M. Di, L. Qin, X. Q. Yao, Y. Z. Li, Z. J. Guo and H. G. Zheng, *Cryst. Growth Des.*, 2012, **12**, 3957-3963.
10. M. D. Zhang, L. Qin, H. T. Yang, Y. Z. Li, Z. J. Guo and H. G. Zheng, *Cryst. Growth Des.*, 2013, **13**, 1961-1969.
11. W. Li, H. P. Jia, Z. F. Ju and J. Zhang, *Cryst. Growth Des.*, 2006, **6**, 2136-2140.
12. J. S. Hu, Y. J. Shang, X. Q. Yao, L. Qin, Y. Z. Li, Z. J. Guo, H. G. Zheng and Z. L. Xue, *Cryst. Growth Des.*, 2010, **10**, 2676-2684.
13. J. Zhang, R. Liu, P. Feng and X. Bu, *Angew. Chem., Int. Ed.*, 2007, **46**, 8388-8391.
14. Bruker (2000 and 2008). APEX and APEX2, SAINT and SADABS. Bruker AXS Inc., Madison, Wisconsin, USA.
15. G. M. Sheldrick, *Shelextl* (Version 6.10), Bruker AXS Inc., Madison, Wisconsin, USA, 2002.
16. V. A. Blatov, A. P. Shevchenko and V. N. Serezhkin, *J. Appl. Crystallogr.*, 2000, **33**, 1193-1193.
17. G. M. Sheldrick, *Acta. Cryst. Sect. A*, 2008, **64**, 112-122.
18. M. Li, D. Li, M. O'Keeffe and O. M. Yaghi, *Chem. Rev.*, 2014, **114**, 1343-1370.
19. A. Blatov, *Struct. Chem.*, 2012, **23**, 955-963.
20. A. L. Spek, *Acta. Cryst. Sect. A*, 1990, **46**, 194-201.
21. J. Yang, J. F. Ma, S. R. Batten and Z. M. Su, *Chem. Commun.*, 2008, 2233-2235.
22. L. Qin, J. Hu, M. Zhang, Y. Li and H. Zheng, *Cryst. Growth Des.*, 2012, **12**, 4911-4918.
23. J. Xu and M. D. Chen, *Chin. J. Inorg. Chem.*, 2013, **29**, 2666-2672.
24. M. Liang and J. Chen, *Chem. Soc. Rev.*, 2013, **42**, 3453-3488.
25. Y. Liu, G. Li, X. Li and Y. Cui, *Angew. Chem. Int. Ed.*, 2007, **46**, 6301-6304.
26. Y. Liu, X. Xu, F. Zheng and Y. Cui, *Angew. Chem. Int. Ed.*, 2008, **47**, 4538-4541.
27. K. Jain and G. W. Pratt, *Appl. Phys. Lett.*, 1976, **28**, 719-721.
28. C. Wang, T. Zhang and W. Lin, *Chem. Rev.*, 2012, **12**, 1084-1104.
29. W. Zhang and R. G. Xiong, *Chem. Rev.*, 2012, **112**, 1163-1195.
30. S. Horiuchi and Y. Tokura, *Nat. Mater.*, 2008, **7**, 357-366.
31. H. Zhao, Z. R. Qu, Q. Ye, B. F. Abrahams, Y. P. Wang, Z. G. Liu, Z. L. Xue, R. G. Xiong and X. Z. You, *Chem. Mater.*, 2003, **15**, 4166-4168.
32. J. F. Scott, *J. Phys.: Condens. Matter*, 2008, **20**, 021001-021002.
33. Y. Cui, Y. Yue, G. Qian and B. Chen, *Chem. Rev.*, 2012, **112**, 1126-1162.
34. D. S. Seneviratne, M. J. Uddin, V. Swayambunathan, H. B. Schlegel and J. F. Endicott, *Inorg. Chem.*, 2002, **41**, 1502-1517.
35. F. N. Castellano, M. Henryk, I. Gryczynski and J. R. Lakowicz, *Inorg. Chem.*, 1997, **36**, 5548-5551.